Optimal Specificity of Thallium-201 SPECT Through Recognition of Imaging Artifacts

E. Gordon DePuey and Ernest V. Garcia

Department of Radiology, Emory University School of Medicine, Atlanta, Georgia

Artifacts are produced in ^{201}Tl cardiac single photon emission computed tomography (SPECT) imaging because of a variety of causes including soft-tissue attenuation, overlying abdominal viscera, variable myocardial thickness, left bundle branch block, cardiac rotation, patient motion, and technical errors. Careful attention to quality control, utilization of motion detectors, and familiarization with potential artifacts will improve the specificity and diagnostic accuracy of ^{201}Tl SPECT for coronary artery disease.

J Nucl Med 30:441–449, 1989

Compared to planar thallium-201 (^{201}Tl) myocardial imaging, single photon emission computed tomography (SPECT) has provided a more sensitive noninvasive means to detect coronary artery disease (CAD) (*1–6*). As a result of SPECT's higher image contrast resolution and its ability to separate overlying myocardial structures, individual coronary vascular territories can be differentiated. Two-dimensional representation of three-dimensional tomographic data by means of polar coordinate, or "bulls-eye", maps has facilitated identification of myocardial perfusion abnormalities (*5*). Quantitative techniques whereby patient data are compared to gender-matched normal files consisting of data from individuals with a low likelihood of coronary disease partly compensate for the current lack of corrections for scattering, variable attenuation, and partial volume effects. This compensation further enhances the identification of perfusion abnormalities and allows for the relative quantification of such defects (*5*).

Despite the improved sensitivity afforded by ^{201}Tl SPECT, there is a need to recognize potential artifacts that are unique to SPECT as well as common to both SPECT and planar imaging in order to obtain optimal specificity. By recognition of such artifacts, the number of patients referred to cardiac catheterization because of "false-positive" ^{201}Tl scans can be minimized, thereby reducing both hospital costs and patient morbidity. There are other factors which also affect the specificity of ^{201}Tl SPECT (as well as any other test) such as the patient selection bias (*7*), angiographic underestimation of the actual hemodynamic effect of coronary lesions, small vessel disease not detectable angiographically, and coronary spasm (*8–10*). Since such factors are usually beyond the control of the nuclear diagnostician, currently the best approach to ensure optimal specificity is to learn to recognize the artifacts that are described in this article.

Common artifacts that we have encountered in ^{201}Tl cardiac SPECT are listed in Table 1. These artifacts have been observed using a 3.5-mCi dose of thallium injected at peak exercise, a 180° imaging arc (45° right anterior oblique to 45° left posterior oblique acquisition), 32 planar acquisitions each for 40 sec at every 5.6° of the imaging arc, a 400-mm field-of-view camera (General Electric 400A, General Electric, Milwaukee, WI) equipped with an all-purpose, parallel hole collimator, filtered backprojection reconstruction using a two-dimensional Ramp-Hanning filter with a 0.822 cycles/cm cutoff frequency and quantification using the Emory bulls-eye program (*5*). We would expect to observe these artifacts using any commercial SPECT equipment, either a 180° or 360° orbit acquisition, and other relative quantification approaches.

Soft-Tissue Attenuation

Filtered backprojection results in areas of apparently decreased myocardial count density underlying areas of increased soft-tissue thickness or density. The most common of these soft-tissue attenuators is the left breast. The count density of the anterior wall of the left ventricle in tomographic myocardial images is lower for women than for men (anterior/inferior count density ratio = 1.2:1 for men and 1.0:1 for women) (*5*). These ratios were derived from an average middle class white population studied at Emory University Hospital.

For reprints contact: E. Gordon DePuey, MD, Emory University Hospital, Dept. of Radiology, 1364 Clifton Rd. NE., Atlanta, GA 30322.

TABLE 1
Thallium-201 SPECT Artifacts

- Soft-tissue attenuation
  - Breasts
  - Lateral chest wall fat
  - Diaphragm
- Overlying visceral activity
- Myocardial "hot spots"
- Apical variations
- Noncoronary disease
  - LBBB
  - Myocardial hypertrophy
  - Dextrorotation/levorotation
- Patient motion
- Oblique axis and bulls-eye reconstruction errors
- Center or rotation errors
- Flood field nonuniformity

However, in women with unusually large or dense breasts, attenuation of the anterior wall is more marked. The location of the resultant scan artifact will depend upon the position of the breast. For instance, in women with firm breasts that lie on the anterior chest wall with the patient supine, the attenuation effect will be most marked over the anterior wall of the left ventricle. In contrast, in women with large, pendulous breasts that lie adjacent to the lateral chest wall the lateral myocardial wall will be more markedly attenuated. If such a patient is wearing a bra, the breasts will be thicker and more anteriorly positioned and will create a more discrete artifact (Fig. 1). Therefore, we routinely image women with their bras removed. In women with breast implants, which are more dense than normal breast tissue, the anterior attenuation artifact is more marked. In men with gynecomastia anterior attenuation artifacts may also occur, and these may be particularly pronounced when patient data are compared with a normal male file.

In contrast to women with large breasts, those with very small breasts and women who have undergone mastectomy have little, if any, anterior myocardial wall attenuation. In such cases count density distribution is similar to that of a normal male, with inferior count density relatively decreased. Therefore, when compared with the normal female file, count density of the inferior wall will appear abnormally decreased (Fig. 2). Thus, in women who have undergone left mastectomy, we routinely compare patient data to the normal male file.

In obese patients there may be considerable accumulation of adipose tissue in the lateral chest wall. When such an individual lies supine, the soft-tissue thickness of the lateral chest wall is further accentuated. In ^{201}Tl SPECT imaging this increase in lateral chest wall density may result in an apparent fixed lateral wall perfusion defect (Fig. 3A).

In both men and women there is a decrease in myocardial count density of the inferior wall compared to the remainder of the myocardium. This is most likely a result of attenuation by the left hemidiaphragm and also the overlying right ventricle and right ventricular blood pool. Such artifacts have already been reported for planar ^{201}Tl imaging (*11*). In patients with abdominal protuberance or left hemidiaphragmic elevation, attenuation of the inferior wall is accentuated. This

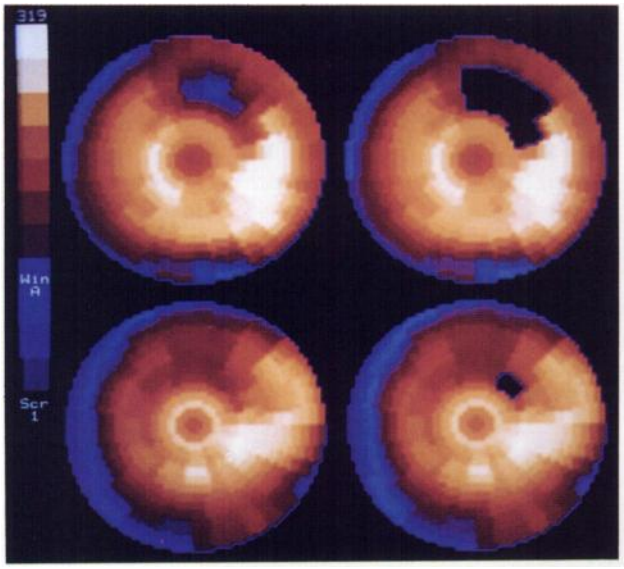

FIGURE 1
Bulls-eye polar coordinate maps reconstructed from ^{201}Tl SPECT images obtained 3 hr postexercise in a woman with a 42-in. chest circumference with her bra on (top left) and immediately thereafter with her bra off (bottom left). Bulls-eye plots in which pixels more than 2.5 s.d.s below mean normal limits are blackened are displayed to the right. See text for explanation.

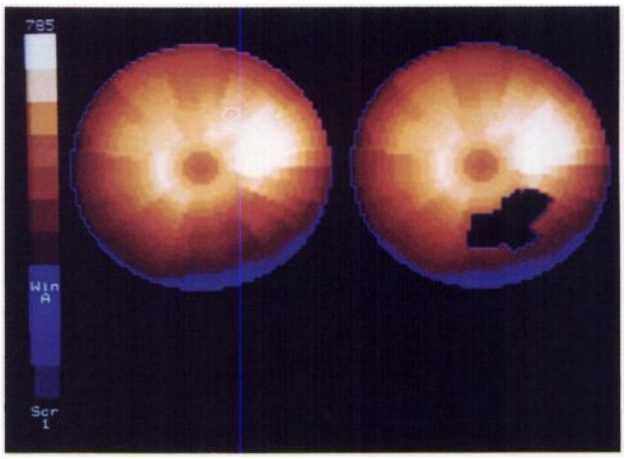

FIGURE 2
Immediate postexercise bulls-eye plot (left) from a woman with normal coronary arteries who had undergone prior bilateral mastectomies. Patient data are compared to the normal female file in the standard deviation blackout plot to the right. See text for explanation.

effect also has been described in patients with ascites secondary to peritoneal dialysis (*12*).

Assuming that patient positioning for immediate and delayed SPECT is identical, all of the above soft-tissue attenuation artifacts will appear fixed, thus mimicking myocardial scarring. However, the artifact may mimic ischemia if soft-tissue attenuation is less in the delayed images. Such a pattern would likely occur in the case of a female patient who was imaged with her bra on for the immediate images but without the bra for the delays.

To increase the awareness of the potential for such soft-tissue attenuation artifacts, it is recommended that the following patient information be routinely recorded and reviewed during scan interpretation: (a) sex, (b) height, (c) weight, (d) chest circumference, (e) bra cup size, (f) history of mastectomy, and (g) history of breast implants. Also, the technologist performing the study records pertinent information about the patient's body habitus (pendulous, laterally positioned breasts, abdominal protuberance, etc). For the physician interpreting the scan, inspection of the multiple planar acquisitions, preferably in dynamic closed-loop "movie-mode" format is very helpful. In women with large or dense breasts, a "shadow" is observed to partially or totally eclipse the myocardium. Similarly, in patients with excessive lateral chest wall fat, the myocardium appears to fade dramatically in the left lateral and left posterior oblique views (Fig. 3B).

Overlying Abdominal Visceral Activity

Whereas there is minimal abdominal visceral ^{201}Tl localization in patients who achieve adequate exercise and shunt blood flow from the abdominal viscera to the peripheral vasculature, in patients undergoing resting ^{201}Tl studies, in those individuals achieving suboptimal peak heart rates, and in those in whom dipyridamole is substituted for exercise, visceral tracer uptake may be significant. In patients with left hemidiaphragmatic elevation or eventration, such tracer avid visceral structures may be superimposed upon the inferior left ventricular myocardium in some of the planar projections. Tomographic reconstruction results in an apparent increase in count density in myocardial regions underlying the visceral activity (Fig. 4). When tomographic slices and/or polar coordinate plots are displayed, they are normalized to the region of the myocardium with the greatest count density, making the remainder of the myocardium appear to have relatively decreased count density. Since in exercise studies visceral activity increases in delayed images, artifacts are more likely to appear in delayed images, mimicking "reverse redistribution." In contrast, in dipyridamole studies where visceral activity is more marked in immediate images, artifacts are more likely to appear in immediate images and resolve in delayed images, thus mimicking myocardial ischemia. Such artifacts due to superimposition of tracer-avid visceral structures are easily identified by inspection of the rotating planar images (Fig. 4).

Myocardial "Hot Spots"

Myocardial count density is occasionally increased in the region of the anterior and posterior papillary muscles. This effect may be attributed in part to a regional increase in myocardial thickness, since for a wall thinner than twice the system's spatial resolution, the observed maximum count density is approximately proportional to thickness (*13,14*). This effect may be

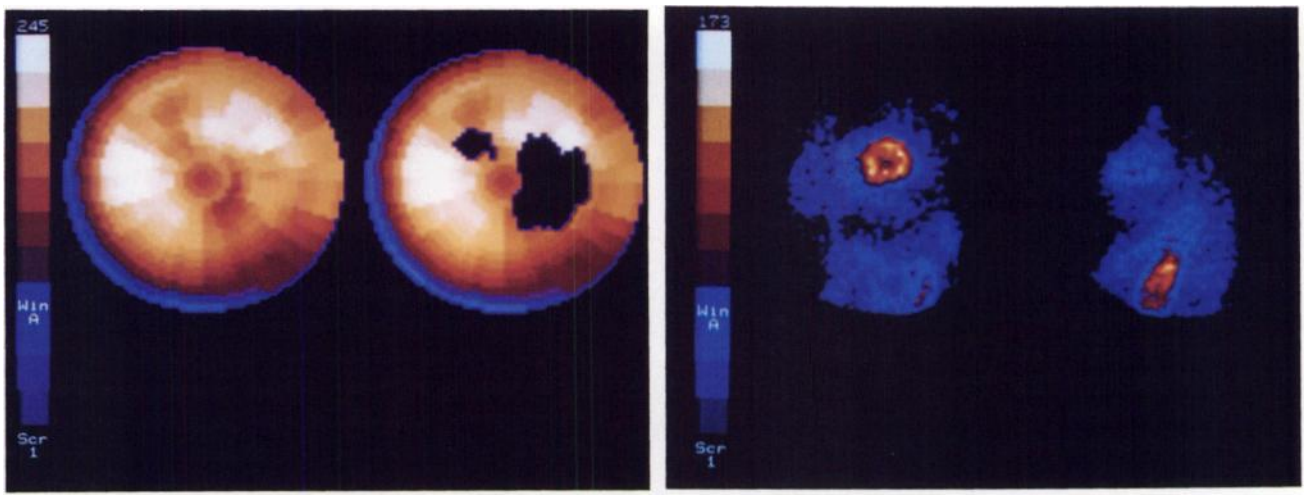

FIGURE 3
Left: Immediate postexercise bulls-eye plot (left) and standard deviation blackout plot (right) in an obese male patient with normal coronary arteries. His chest circumference is 50 in. with considerable accumulation of adipose tissue in the lateral chest walls. See text for explanation. Right: Forty-five degree left anterior oblique (left) and left lateral (right) planar images obtained from the rotating planar display. In the left lateral view there is marked attenuation of myocardial activity by lateral chest wall soft tissue.

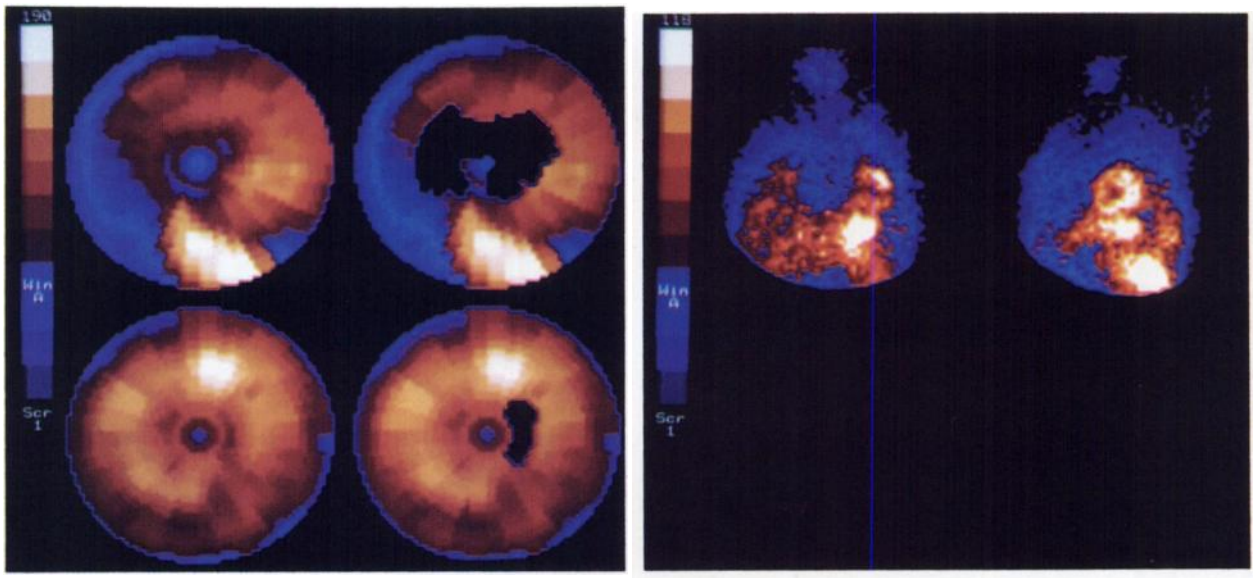

FIGURE 4
Left: Bulls-eye plots (left) and standard deviation blackout plots (right) obtained immediately following intravenous dipyridamole infusion (top) and at a 4-hr delayed interval (bottom). In the immediate images there is an apparent marked increase in tracer concentration in the inferior wall of the left ventricle (6 o'clock) due to superimposition of splenic activity. Since the image is normalized to the area of greatest tracer concentration, the remainder of the ventricle remains count-poor and is identified as abnormal in the standard deviation blackout plot. At 4 hr, after tracer has washed out of the spleen, the inferior artifact is no longer present, and the image appears normal. This artifact mimics extensive ischemia of the septum, anterior, and lateral walls. Right: Anterior (left) and 60° left anterior oblique (right) planar images obtained from the rotating planar display. Marked splenic tracer concentration is present below the heart and contiguous with the inferior wall of the left ventricle.

more marked in patients with left ventricular hypertrophy. Infrequently, localized "hot spots" may also be seen in the apex or other myocardial regions. These cannot be attributed to normal anatomic structures and are currently of unknown etiology. When tomographic myocardial slices and circumferential profile plots are normalized to areas of the greatest myocardial count density, these "hot spots" appear normal, and the remainder of the myocardium appears to have diminished count density. Although such "hot spots" may appear in either immediate postexercise or delayed images, in our experience, they are somewhat more frequent in the former. Therefore, the artifact may appear only in immediate images and thus mimic exercise-induced ischemia.

"Hot spot" artifacts are usually most easily recognized by inspection of tomographic myocardial slices, particularly short axis slices. They are sometimes less obvious on polar coordinate maps (Fig. 5).

Apical Variations

Myocardial count density in the left ventricular apex may be decreased as a result of normal anatomic thinning. In SPECT studies this apical "dimple" is usually noted at the very tip of the apex in horizontal long axis slices. However, it may be displaced laterally or less frequently, towards the septum. In the Emory method of bulls-eye reconstruction, in which the operator selects the apical-most short axis slice, displacement of the apical dimple laterally or septally may create an image artifact (Fig. 6). Careful inspection of horizontal long axis slices alerts the interpreting physician to the position of the apical "dimple" and the potential for such an artifact.

Noncoronary Disease

Left bundle branch block. In dog experiments wherein coronary blood flow has been measured with radioactive microsphere injections, left bundle branch block (LBBB) results in a decrease in coronary blood flow to the interventricular septum (*15*). The decrease in septal blood flow is felt to be a result of asynchronous relaxation of the septum, which is out of phase with diastolic filling of the remainder of the left ventricle, during which time coronary perfusion is maximal. In a study performed at our institution, nine of ten patients with LBBB and angiographically normal coronary arteries demonstrated significant reversible septal perfusion defects with ^{201}Tl SPECT (*16*). These abnormalities were more marked in patients who achieved very high peak heart rates (>170 bpm). We postulated that tracer redistribution into the septum in delayed images occurred because septal asynchrony was less marked at lower resting heart rates. Therefore, it is imperative that the patient's electrocardiogram be inspected for fixed or rate-related LBBB.

Myocardial hypertrophy. In patients with myocardial hypertrophy resulting from longstanding hypertension

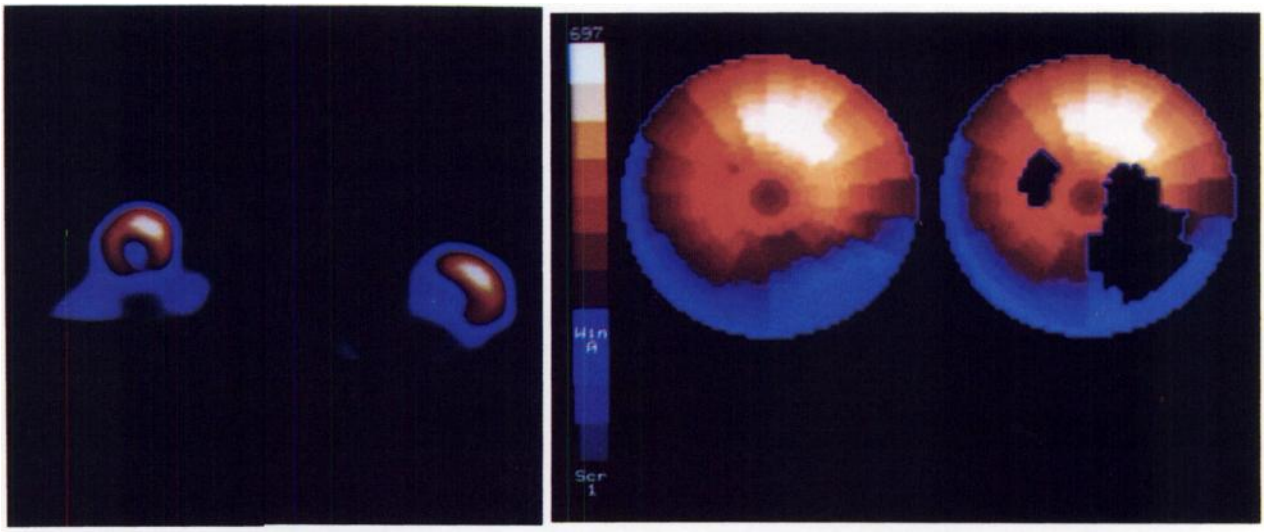

FIGURE 5
Left: Mid-ventricular short axis (left) and vertical long axis (right) oblique tomographic slices demonstrating increased tracer concentration in the anterior wall of the left ventricle in the region of the anterior papillary muscle. The remainder of the myocardium appears relatively count-poor because the images are each normalized to the area of greatest count density. Right: Corresponding bulls-eye plot (left) and standard deviation blackout plot (right) also demonstrate relatively increased tracer concentration in the anterior wall (11 o'clock to 2 o'clock). Since the bulls-eye plot is normalized to the area of greatest count density in the anterior wall, the remainder of the ventricle appears abnormal.

or valvular heart disease, we have observed a relative decrease in lateral myocardial wall count density (*17*). In hypertensive patients the lateral-to-septal count density ratio in immediate ^{201}Tl SPECT images was significantly lower than that in normotensive control subjects (1.02 ± 0.10 vs. 1.17 ± 0.08, $p < 0.00001$). A similar decrease in lateral-to-septal count density ratio was observed in 3-hr delayed images (1.02 ± 0.11 vs. 1.11 ± 0.08, $p < 0.00001$). Usually, the relative decrease in lateral wall count density is similar in immediate and delayed images, thus mimicking myocardial infarction. Therefore, it is important to question patients referred for ^{201}Tl SPECT regarding a history of hypertension, chronic renal disease, or valvular or congenital heart disease. Although inspection of the electrocardiogram for evidence of left ventricular hypertrophy is worthwhile, the standard voltage criteria of left ventricular hypertrophy are relatively insensitive (*18*).

Cardiac dextrorotation/levorotation. An infrequent 180° ^{201}Tl SPECT artifact is alteration in the lateral-to-septal count density ratio in patients with cardiac rotation. In patients with cardiac dextrorotation the septum lies closer to the scintillation camera detector positioned in the right anterior oblique and anterior projections, and the lateral wall lies further from the detector in the lateral and left posterior oblique views. This results in an apparent relative increase in septal count density and a relative decrease in lateral wall count density. This fixed decrease in lateral count density mimics lateral wall myocardial infarction. In contrast, with levorotation the lateral wall is "seen" better in the lateral and left posterior oblique views, and the septum is "seen" less well in the anterior and right anterior oblique views, creating the impression of a fixed septal defect. To investigate this effect, we simulated cardiac rotation by obtaining a 360° acquisition and varying the 180°

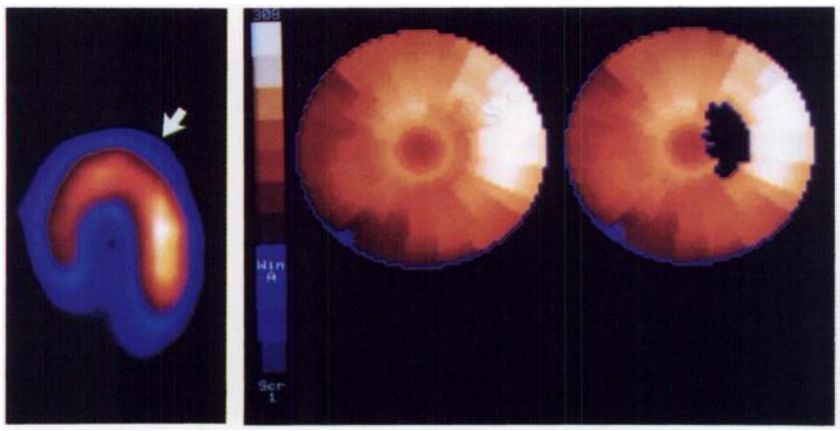

FIGURE 6
Left: Horizontal long axis oblique tomographic slice demonstrating posterolateral displacement of physiologic apical thinning (arrow). Right: Corresponding bulls-eye plot (left) and standard deviation blackout plot (right) demonstrating a comma-shaped defect posteroapically in the region of physiologic thinning.

arc from which the tomographic slices were reconstructed (Fig. 7). There was a progressive decrease in lateral wall count density paralleling the simulated degree of dextrorotation and a progressive decrease in septal count density with levorotation.

Although we have observed this artifact uncommonly, patients with known congenital heart disease, hyperexpansion of the lungs, and marked selective dilatation of either the right or left ventricle should be suspected of having altered cardiac rotation. By inspecting the transaxial myocardial slices, the orientation of the left ventricle within the chest can be assessed. The electrocardiogram may provide additional information. Three-hundred-sixty degree acquisition would most likely minimize this artifact.

Patient Motion

From studies performed at our institutions (*19,20*) and at other centers (*21*), it has been reported that patient motion as little as 3 mm (0.5 pixel) can create ^{201}Tl SPECT image artifacts mimicking perfusion abnormalities. In our experience, in day-to-day clinical studies slight patient motion is tolerable and does not appear to produce significant scan artifacts. With greater patient motion, the appearance of the scan artifact will depend upon the direction of motion, the planar frames in which it occurs, whether the motion is abrupt or gradual, and whether the heart returns to the baseline position. At this time it is unknown what type and degree of motion will routinely cause scan artifacts.

"Diaphragmatic creep" is another type of motion artifact which has been reported (*22*). Immediately postexercise with increased depth of respiration and diaphragmatic flattening, the heart lies low in the thorax. As SPECT image acquisition proceeds, respiration becomes more shallow, and the heart gradually "creeps" upward. In reconstructed SPECT images such "upward creep" results in an apparent decrease in count density in the inferior wall of the left ventricle. Since the artifact is not present in delayed images, obtained when the depth of respiration is constant, the "diaphragmatic creep" artifact mimics inferior ischemia. To avoid diaphragmatic creep these investigators have advocated delaying immediate postexercise image acquisition for 15 min to allow for hyperventilation to subside and the depth of respiration to stabilize.

Cardiac motion during tomographic acquisition is best detected by inspection of the multiple planar acquisitions viewed in dynamic "movie-mode" format. Inspection of the image sinogram may also be helpful. In our experience, the use of chest wall radioactive markers has been of less value and may even create additional scan artifacts. Recently, useful computer algorithms have been introduced to automatically detect and correct for patient motion (*19,20,22*).

Oblique Axis and Bulls-eye Reconstruction Errors

If the long axis of the left ventricle is selected incorrectly from either the mid transaxial or mid vertical long axis slice, the geometry of the ventricle in reconstructed orthogonal slices can be distorted (Fig. 8). With polar coordinate plot reconstruction such distortion most often results in areas of apparently decreased count density in the basal myocardial regions at the periphery of the bulls-eye plot.

With the Emory method of bulls-eye plot reconstruction, the count density of the apex may be underesti-

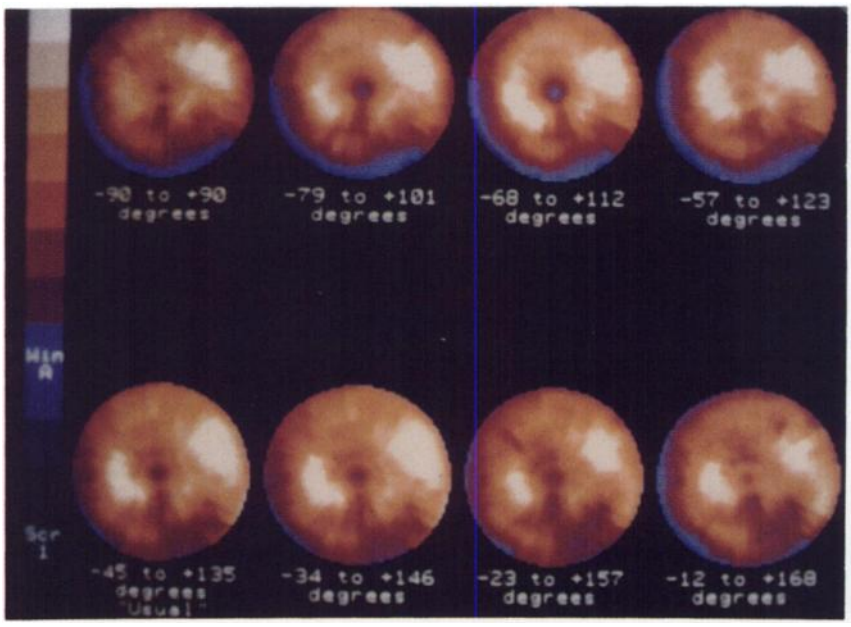

FIGURE 7
The bulls-eye plot obtained in a normal male individual is in the lower left hand corner. Images in which progressive cardiac dextrorotation was simulated by altering the rotational arc used for acquisition are portrayed in the bottom row. Progressive levorotation is portrayed in the upper row (most marked levorotation in upper left image). See text for explanation.

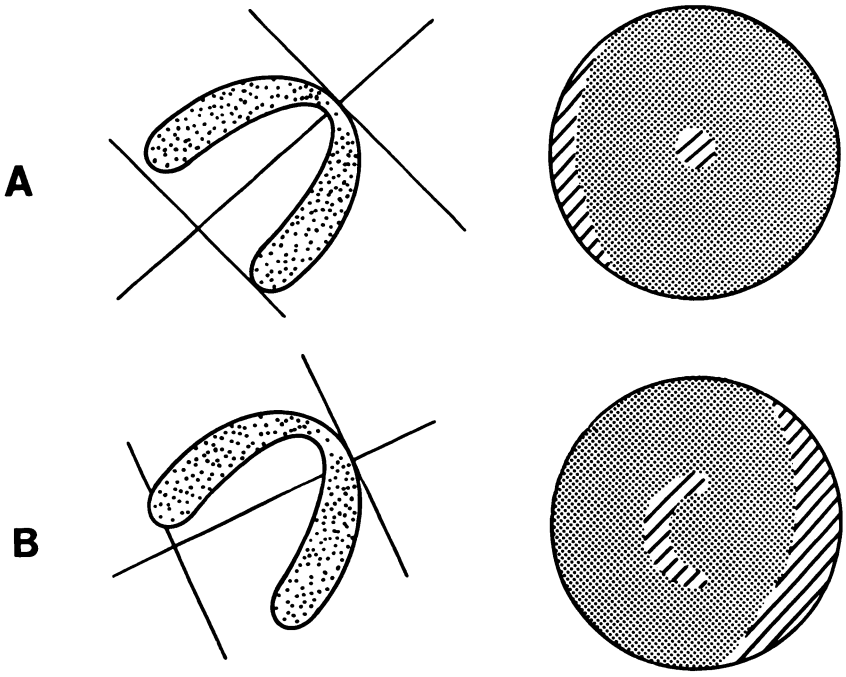

FIGURE 8
A: Correct long axis selection from the diagrammed transaxial tomographic slice results in a bulls-eye image with regions of physiologically decreased count density (cross-hatched areas) at the base of the septum due to the membranous septum, and at the apex due to anatomic thinning. B: With incorrect long axis selection a semilunar artifact is created at the periphery of the lateral wall. The apex is shifted anteriorly, creating a comma-shaped artifact in the septum, corresponding to the region of physiologic apical thinning.

mated or overestimated as a result of incorrect apical slice selection (*5*). If the apical limit of the myocardium is selected too far beyond the actual apex, not enough myocardium will be included in the slice, and the apex will appear to have decreased count density. More frequently, particularly in patients with true apical perfusion defects, the technologist selects the apical slice too far into the heart, thus underestimating the severity and extent of the defect. This problem is minimized in a method developed at Cedars-Sinai Medical Center (*23*) that selects the apical portion of the polar coordinate plot from vertical long axis slices.

Thus, inspection of the axes and limits of myocardium used for oblique tomographic slice reconstruction and polar coordinate map construction is an important part of ^{201}Tl SPECT quality control.

Center of Rotation Errors

Another important aspect of camera quality control performed by the technologist, which is often transparent to the nuclear medicine physician interpreting scans, is the determination of the camera center of rotation used for SPECT image reconstruction. Errors in the center of rotation in the positive (rightward) or negative (leftward) direction create posteroapical or anteroapical artifacts, respectively (Fig. 9). In horizontal long axis tomographic slices, such artifacts appear linear, extending through the thickness of myocardium,

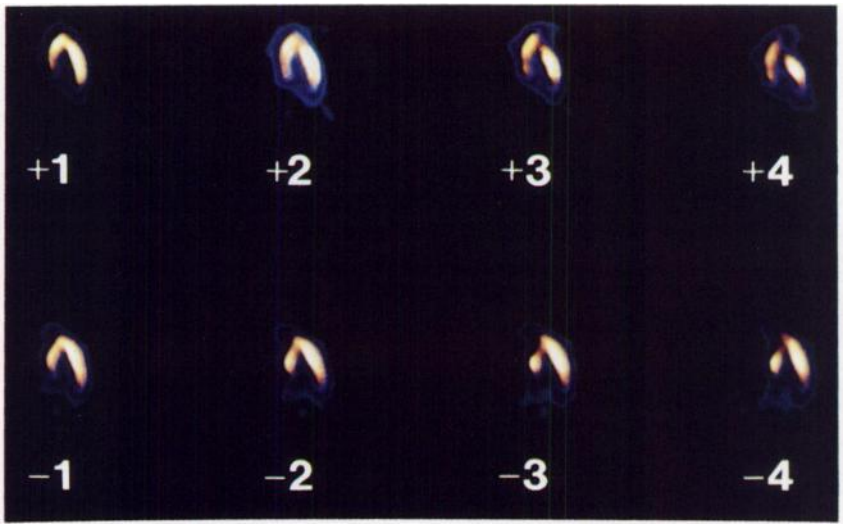

FIGURE 9
Horizontal long axis slices in a normal individual in which the center of rotation was progressively shifted to the right (+1–+4 pixels) and to the left (−1–−4 pixels). With increasing center of rotation artifacts, the septal and lateral walls appear to be misaligned. Rightward (+) center of rotation errors produce linear posteroapical defects, and leftward (−) errors create linear anteroapical defects.

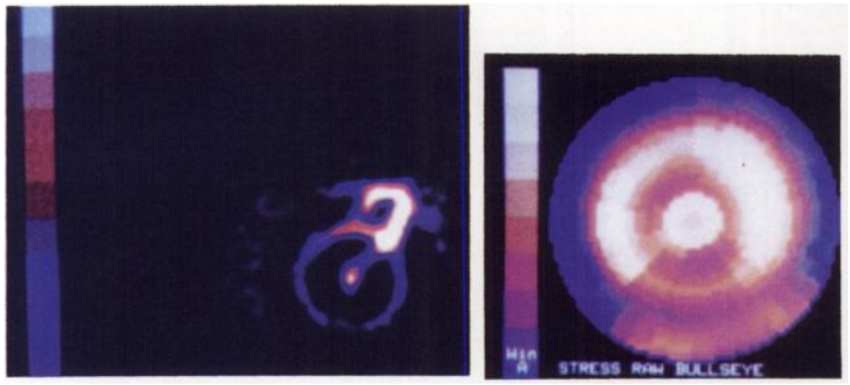

FIGURE 10
Left: Transaxial tomographic slice demonstrating ring artifacts due to marked flood field nonuniformity. The intensity of the images is intentionally increased to accentuate the artifact. Right: Corresponding bulls-eye plot also demonstrating the concentric ring artifact.

and the anterior and posterior walls appear misaligned. In bulls-eye plots such artifacts appear comma-shaped.

Flood Field Nonuniformity

With marked flood field nonuniformity we have observed ring-like artifacts in reconstructed tomographic slices which are also evident in circumferential profile plots. In one extreme example shown in Figure 10, a faulty connection in a detector circuit created severe field nonuniformity resulting in marked ring artifacts. This problem was difficult to detect since the circuit would always function properly when positioned at 180° (facing up). Unfortunately, this is the position we used for performing the field uniformity tests. It should be noted that due to the relatively low counts found in ^{201}Tl SPECT studies, nonuniformities (as evidenced by ring-artifacts) are usually hidden within the statistical noise. Therefore, the appearance of ring-artifacts in these studies implies that there exists a major detector uniformity problem.

TABLE 2
Guidelines to Increase Awareness of Thallium-201 Artifacts

Clinical history
Hypertension, valvular heart disease, renal disease
Breast implants/augmentation
Peritoneal dialysis
Congenital heart disease, emphysema
Physical examination
Sex, height, weight
Chest circumference, bra cup size
Lateral chest wall fat
Abdominal protuberance
Chest wall deformity
Electrocardiogram
Left bundle branch block
Left ventricular hypertrophy
Abnormal left ventricular axis
Rotating planar images
Localized attenuation
Abdominal viscera overlying heart
Patient motion
Oblique tomographic slice inspection
"Hot spots"
Apical "dimple"
Ring artifacts
Left ventricular long axis selected
Slices for polar coordinate map reconstruction
Camera quality control
Center of rotation
Flood field

Summary

With the advent of new correction methods for Compton scattering, variable attenuation, and object size effects (*24–32*) the need to "read around" many of the artifacts described above should be diminished. For now, careful attention to quality control, utilization of motion detection and perhaps motion correction algorithms, and particularly familiarization with potential artifacts should improve the specificity and diagnostic accuracy of ^{201}Tl SPECT for coronary artery disease. Abstracting pertinent information from the patient's clinical history, physical examination, and electrocardiogram, as well as important laboratory control measures are also required.

REFERENCES

1. Tamaki S, Najajima H, Murakami T, Yui Y, Kambara H, Kadota K. Estimation of infarct size by myocardial emission computed tomography with thallium-201 and its relation to creatine kinase-MB release after myocardial infarction in man. *Circ* 1982; 66:994–1001.
2. Caldwell J, Williams D, Richie J. Single photon emission computed tomography: validation and application for myocardial perfusion imaging. In: Pohost G, Higgins C, Morganroth J, Richie J, Shelbert H, eds. *New concepts in cardiac imaging 1985*. Boston: G. K. Hall, 1985: 115–136.

3. Ritchie JL, Williams DL, Harp G, Stratton JL, Caldwell JH. Transaxial tomography with thallium-201 for detecting remote myocardial infarction. *Am J Cardiol* 1982; 50:1236–1241.
4. Caldwell J, Williams D, Harp G, Stratton J, Ritchie J. Quantitation of size of relative myocardial perfusion defect by single-photon emission computed tomography. *Circ* 1984; 70:1048–1056.
5. DePasquale EE, Nody AC, DePuey EG, et al. Quantitative rotational thallium-201 tomography for identifying and localizing coronary artery disease. *Circ* 1988; 77:316–327.
6. Maddahi J, Van Train KF, Wong C, et al. Comparison of thallium-201 SPECT and planar imaging for evaluation of coronary artery disease [Abstract]. *J Nucl Med* 1986; 27:999.
7. Rozanski A, Diamond GA, Berman D, et al. The declining specificity of exercise ventriculography. *N Engl J Med* 1983; 309:518–522.
8. Ziflstra F, Fioretti P, Reiber JHC, Serruys PW. Which cineangiographically assessed anatomic variable correlates best with functional measurements of stenosis severity? A comparison of quantitative analysis of the coronary flow reserve and exercise/redistribution thallium-201 scintigraphy. *J Am Coll Cardiol* 1988; 12: 686–691.
9. Vogel RA. Assessing stenosis significance by coronary arteriography: are the best variables good enough? *J Am Coll Cardiol* 1988; 12:692–693.
10. Fuller CM, Raizner AE, Chahine RA, et al. Exercise induced coronary artery spasm: angiographic demonstration, documentation of ischemia by myocardial scintigraphy and results of pharmacologic intervention. *Am J Cardiol* 1980; 46:500–506.
11. Johnstone D, Wakers F, Berger H, et al. Effect of patient positioning on left lateral thallium-201 myocardial images. *J Nucl Med* 1979; 20:183–188.
12. Rab ST, Alazraki N, Krawczynska EG. Peritoneal fluid causing inferior attenuation on SPECT thallium-201 myocardial imaging in women. *J Nucl Med* 1988; 29: 1860–1864.
13. Hoffman EJ, Huang SC, Phelps ME. Quantitation in positron emission computed tomography. 1. Effect of object size. *J Comput Assist* 1979; 3:299–308.
14. Galt JR, Robbins WL, Eisner RL, Garcia EV. Thallium-201 myocardial SPECT quantitation: effect of wall thickness [Abstract]. *J Nucl Med* 1987; 27:577.
15. Hirzel HO, Senn M, Nuesch K, et al. Thallium-201 scintigraphy in complete left bundle branch block. *Am J Cardiol* 1984; 53:764–769.
16. DePuey EG, Guertler-Krawczynska E, Robbins WL. Thallium-201 SPECT in coronary artery disease patients with left bundle branch block. *J Nucl Med* 1988; 29:1479–1485.
17. DePuey EG, Guertler-Krawczynska E, Perkins JV, Robbins WL, Whelchel JD, Clements SD. Alterations in myocardial thallium-201 distribution in patients with chronic systemic hypertension undergoing single-photon emission computed tomography. *Am J Cardiol* 1988; 62:234–238.
18. Devereux RB, Alonso DR, Lutas EM, et al. Echocardiographic assessment of left ventricular hypertrophy: comparison of necropsy findings. *Am J Cardiol* 1986; 57:450–458.
19. Eisner RL, Noever T, Nowak D, et al. Use of cross-correlation function to detect patient motion during SPECT imaging. *J Nucl Med* 1987; 28:97–101.
20. Eisner R, Churchwell A, Noever T, et al. Quantitative analysis of the tomographic thallium-201 myocardial bullseye display: critical role of correcting for patient motion. *J Nucl Med* 1988; 29:91–97.
21. Friedman J, Berman DS, Van Train K, et al. Patient motion in thallium-201 myocardial SPECT imaging. An easily identified frequent source of artifactual defect. *Clin Nucl Med* 1988; 13:321–324.
22. Geckle WJ, Frank TL, Links JM, Becker LC. Correction for patient and organ movement in SPECT: application to exercise thallium-201 cardiac imaging [Abstract]. *J Nucl Med* 1986; 27:899.
23. Garcia E, Van Train K, Maddahi J, et al. Quantification of rotational thallium-201 myocardial tomography. *J Nucl Med* 1985; 26:17–26.
24. Oppenheim BE. Scatter correction for SPECT. *J Nucl Med* 1984; 25:928–929.
25. Axelsson B, Msaki P, Israelsson A. Subtraction of Compton-scattered photons in single photon emission computerized tomography. *J Nucl Med* 1984; 25:490–494.
26. Floyd CE, Jaszczak RJ, Harris CC, Coleman RE. Energy and spatial distribution of multiple order Compton in SPECT: a Monte Carlo investigation. *Phys Med Biol* 1984; 29:1217–1230.
27. Jaszczak RJ, Greer KL, Floyd CE, Harris CC, Coleman RE. Improved SPECT quantification using compensation for scattered photons. *J Nucl Med* 1984; 25:893–900.
28. Chang LT. A method for attenuation correction in radionuclide computed tomography. *IEEE Trans Nucl Sci NS* 1978; 25:638–643.
29. Galt JR, Hamilton DR, Garcia EV. Attenuation correction equations for SPECT [Letter]. *J Nucl Med* 1987; 28:1925.
30. Bailey DL, Hutton BF, Walker PJ. Improved SPECT using simultaneous emission and transmission tomography. *J Nucl Med* 1987; 28:844–851.
31. Manglos SH, Jaszczak RJ, Floyd CE, Hahn LJ, Greer KL, Coleman RE. Nonisotropic attenuation in SPECT: phantom tests of quantitative effects and compensation techniques. *J Nucl Med* 1987; 28:1584–1591.
32. Galt JR, Hamilton DR, Garcia EV. SPECT quantitation: attenuation correction in inhomogenous media utilizing a transmission scan and assigned attenuation coefficients [Abstract]. *J Nucl Med* 1988; 29:797.